J Biosci (2019) 44:82
DOI: 10.1007/s12038-019-9916-0

Real-time monitoring of translocation of selected type-III effectors from *Xanthomonas oryzae* pv. *oryzae* into rice cells

HUIJIE BIAN[1], LIYUAN ZHANG[2], LEI CHEN[2], WENZHAN WANG[1], HONGTAO JI[3]* and HANSONG DONG[1,2]*

[1]*Department of Plant Pathology, Nanjing Agricultural University, Nanjing 210095, Jiangsu Province, People's Republic of China*

[2]*Department of Plant Pathology, Shandong Agricultural University, Taian 210016, Shandong Province, People's Republic of China*

[3]*Department of Biology, Jiangsu Normal University, Xuzhou 221116, Jiangsu Province, People's Republic of China*

**Corresponding author (Email, 6020160135@jsnu.edu.cn; hsdong@njau.edu.cn)*

MS received 10 February 2019; accepted 12 May 2019; published online 2 August 2019

Type-III (T3) effectors PthXo1 and AvrXa10 of *Xanthomonas oryzae* pv. *oryzae* are translocated into rice cells to induce virulence and avirulence on susceptible- and resistant-rice varieties Nipponbare and IRBB10, respectively. The translocation needs the bacterial T3 translocator Hpa1 and rice *Oryza sativa* plasma membrane protein OsPIP1;3. Here, we employed the β-lactamase (BlaM) reporter system to observe PthXo1 and AvrXa10 translocation. The system was established to monitor effectors of animal-pathogenic bacteria by quantifying the BlaM hydrolysis product [P] and fluorescence resonance energy transfer (FRET) of the substrate. The feasibility of the BlaM reporter in rice protoplasts was evaluated by three criteria. The first criterion indicated differences between both [P] and FRET levels among wild types and *OsPIP1;3*-overexpressing and *OsPIP1;3*-silenced lines of both Nipponbare and IRBB10. The second criterion indicated differences between [P] and FRET levels in the presence and absence of Hpa1. The last criterion elucidated the coincidence of PthXo1 translocation with induced expression of the PthXo1 target gene in protoplasts of Nipponbare and the coincidence of AvrXa10 translocation with induced expression of the AvrXa10 target gene in protoplasts of IRBB10. These results provide an experimental avenue for real-time monitoring of bacterial T3 effector translocation into plant cells with a pathological consequence.

Keywords. β-lactamase (BlaM) reporter; translocation; type-III (T3) effectors

Abbreviations: BlaM, β-lactamase; PIP, plasma membrane intrinsic protein; PM, plasma membrane; TAL, translocation activator-like; T3, type III; *Xoo*, *Xanthomonas oryzae* pv. *oryzae*

1. Introduction

Many Gram-negative bacteria, either plant (Alfano and Collmer 2004; White *et al.* 2009) or animal (Chatterjee *et al.* 2013) pathogens, use the type-III (T3) secretion system to secrete effector proteins. Then, effectors are translocated from bacterial cells into the cytosol of eukaryotic cells to fulfill a virulent or an avirulent role depending on the host susceptibility (Bogdanove and Voytas 2011; Zhang *et al.* 2015; Chen *et al.* 2017; Wang *et al.* 2018). Three models have been proposed regarding regulation schemes of T3 effector translocation. The first model is translocon-independent pore formation (Domingues *et al.* 2016; Schreiber *et al.* 2016) and the second model is translocon-independent endocytosis possibly by membrane protein trafficking (Kikuchi *et al.* 2016; Gu *et al.* 2017). The third model is the canonical T3 translocon, which hypothetically consists of hydrophilic and hydrophobic protein translocators from bacteria on one hand (Ji and Dong 2015a; Wang *et al.* 2018). On the other, the distinct translocators assemble the sophisticated translocon theoretically by complicated monogenous and heterogeneous molecular interactions and by associations with specific recognizers of translocators situated at plasma membranes (PMs) of eukaryotic cells

Electronic supplementary material: The online version of this article (https://doi.org/10.1007/s12038-019-9916-0) contains supplementary material, which is available to authorized users.

(Büttner 2012; Ji and Dong 2015a, b). To date, independent studies on three models have obtained empirical genetic evidence (Finsel and Hilbi 2015; Domingues *et al.* 2016; Dong *et al.* 2016; Scheibner *et al.* 2017), but relationship of different effectors to any of the models is under debate.

All hydrophilic components of T3 translocators so far identified in plant-pathogenic bacteria are characteristic of harpins, which belong to T3 accessory proteins required for pilus growth or translocon formation (Kvitko *et al.* 2007; Bocsanczy *et al.* 2008; Wang *et al.* 2018). These T3 accessory proteins fall into two categories: one-domain harpins that contain a unitary hydrophilic domain, and two-domain harpins that carry an additional lytic transglycosylase or a pectate lyase enzymatic domain in direct ligation with the upstream hydrophilic sequence (Choi *et al.* 2013; Dik *et al.* 2017). This structural difference makes one-domain and two-domain harpins distinct from each other in the subcellular localization and molecular recognition during bacterial infection in plants. While two-domain harpins may target the bacterial periplasm or plant cell walls to facilitate pilus growth (Charkowski *et al.* 1998; Kim and Beer 1998), one-domain harpins localize to plant PMs, with a potential role in the translocon assembly (Bocsanczy *et al.* 2008; Haapalainen *et al.* 2011; Wang *et al.* 2018). Specific recognizers, lipidic or proteic compounds located at eukaryotic PMs, are supposed to be indispensable for translocator recognition and translocon formation (Chatterjee *et al.* 2013; Ji and Dong 2015a).

The aquaporin of *Oryza sativa*, PM intrinsic protein OsPIP1;3, is implicated in the recognition of the one-domain harpin Hpa1 produced by *Xanthomonas oryzae* pv. *oryzae* (*Xoo*), the pathogen that causes bacterial blight in rice (Zhu *et al.* 2000). Hpa1 is a hydrophilic protein (Chen *et al.* 2008) and a virulence factor (Zhu *et al.* 2000; Wang *et al.* 2018). In rice plants under infection by *Xoo*, secreted Hpa1 serves as a translocator for at least two transcription activator-like (TAL) effectors (TALEs), AvrXa10 and PthXo1, secreted by *Xoo* strains PXO86 and PXO99, respectively (Wang *et al.* 2018). AvrXa10 is an avirulence effector, conferring resistance by activating the host resistance gene *Xa10* in the resistant *indica* rice variety IRBB10 (Tian *et al.* 2014). By contrast, PthXo1 induces virulence by activating the host susceptibility gene *SWEET11* (synonym *Os8N3*) in the susceptible *japonica* rice variety Nipponbare (Yang *et al.* 2006). Nipponbare is susceptible to PXO99^{A}, a well-studied *Xoo* strain (Yang *et al.* 2006; Wang *et al.* 2018; Zhang *et al.* 2018). To infect Nipponbare, PXO99^{A} secretes Hpa1 and delivers it on the interface, where Hpa1 acts to mediate translocation of subsequently secreted PthXo1 into Nipponbare cells (Wang *et al.* 2018). Then, PthXo1 induces virulence by activating the host susceptibility gene *OsSWEET11* (Yang *et al.* 2006) in an OsPIP1;3-dependent manner (Zhang *et al.* 2018). If *OsPIP1;3* is silenced, PthXo1 translocation and *OsSWEET11* expression incur concomitant impairments, alleviating virulence as a consequence (Zhang *et al.* 2018).

Accurate assessment of T3 effector translocation is critical to evaluate the virulence or avirulence roles of an effector, and is particularly important for further elucidating the regulation models. A widely used conventional method is the calmodulin-dependent adenylate cyclase (Cya) reporter assay. Cya generates cyclic adenosine monophosphate (cAMP) as the exclusive product in eukaryotic cells and cAMP concentrations represent amounts of a Cya-fused prokaryotic effector moved into eukaryotic cells (Chakravarthy *et al.* 2017; Wang *et al.* 2018; Zhang *et al.* 2018). The presence of an effector-Cya fusion protein in eukaryotic cells can be detected by immunoblotting (western blotting) with the specific anti-Cya antibody (Wang *et al.* 2018; Zhang *et al.* 2018). In contrast to the static analysis using the Cya reporter, a real-time yet high-throughput technique has been provided by the β-lactamase (BlaM) reporter system (Jones and Padilla-Parra 2016), initially developed for animal-pathogenic bacteria (Mills *et al.* 2008, 2013). The BlaM reporter system involves the infection of eukaryotic cells prelabeled with CCF2, a BlaM hydrolytic substrate that is composed of a cephalosporin core linking two fluorophores and is located in the eukaryotic cytoplasm. Without hydrolysis by an effector-BlaM fusion protein, CCF2 undergoes fluorescence resonance energy transfer (FRET), thus emitting a green fluorescence in a wavelength range of 520–535 nm. Translocated effector-BlaM cleaves CCF2 and disrupts FRET, thus resulting in a blue emission within a wavelength range of 447–465 nm, and the CCF2 cleavage product [P] can be used to indirectly quantify the translocated effector (Mills *et al.* 2008; Jones and Padilla-Parra 2016).

Here, we choose *Xoo* TALEs PthXo1 and AvrXa10 to assess the feasibility of the BlaM reporter in monitoring of T3 effector translocation from plant-pathogenic bacteria to cells of host plants. PthXo1 is originally present in PXO99^{A} while AvrXa10 is *de novo* produced in PXO99^{A} after transformation with the *avrXa10* gene from PXO86. In Cya reporting assay, PthXo1 and AvrXa10 are translocated into the cells of Nipponbare and IRBB10 to induce virulence (including *OsSWEET11* expression) and avirulence (including *Xa10* expression), respectively (Wang *et al.* 2018). As HrcU is an inner membrane protein essential for substrate docking into the T3 secretion system in *Xanthomonas* bacteria (Hartmann and Büttner 2013), the recombinant PXO99^{A} strain Δ*hrcU/TALE-cya* has been used as a negative control in the Cya reporting assay (Wang *et al.* 2018). Similarly, the recombinant PXO99^{A} strain Δ*hrcU/TALE-blaM* will also be used in BlaM reporter assays. The feasibility of the BlaM reporter in rice protoplasts will be evaluated by three criteria, applied to [P] levels and FRET signals as essential parameters of the reporter system. The first criterion is differences between both parameters among the wild-type (WT) Nipponbare plants as well as *OsPIP1;3*-overexpressing transgenic line *OsPIP1;3*OE36 and *OsPIP1;3*-silenced line *OsPIP1;3*i1, which were generated under the Nipponbare background in our previous study

(Zhang *et al.* 2018). *OsPIP1;3*OE and *OsPIP1;3*i lines were also generated under the IRBB10 background, which was not reported and will be documented in this article. The second criterion is differences between [P] levels and FRET signals in the presence and absence of Hpa1. The last criterion is the coincidence of PthXo1 translocation with induced expression of the PthXo1 target gene (*OsSWEET11*) in protoplasts of Nipponbare and the coincidence of AvrXa10 translocation with induced expression of the AvrXa10 target gene (*Xa10*) in protoplasts of IRBB10.

2. Materials and methods

2.1 *Plant growth and bacteria culture*

Rice seeds were germinated in flat plastic trays filled with a substrate containing peat, sand and vermiculite (1:1:1 v/v). Three days later, the germinal seedlings were moved into 12 L pots (two plants per pot) filled with soil from a local rice-grower field. Seeds were incubated and the plants were grown in environment-controlled chambers under 28°C, 12 h light at 250 ± 50 μmol quanta/m^2/s and a relative humidity of 85%. Bacteria (supplementary table 1) were cultured at 28°C on nutrient broth (NB) or nutrient agar (NA) medium (Li *et al.* 2011).

2.2 *Xoo gene modifications*

The *hpa1* and *pthXo1* genes were deleted from $PXO99^A$ by using the unmarked deletion method (Li *et al.* 2011). Upstream and downstream flanking partial sequence fragments of *hpa1* or *pthXo1* were amplified from the $PXO99^A$ genomic DNA and connected together by overlapped fusion-polymerase chain reaction (PCR) using specific primers. Every PCR product was confirmed by sequencing and then cloned into the vector pK18*sacB* by digestion with *Bam*HI and *Xba*I and ligation with T4 ligase (Thermo Scientific). Every recombinant vector was introduced into $PXO99^A$ cells by electroporation, followed by single-colony selection on kanamycin-containing and sugar-free NA plates. Colonies from single crossovers were transferred to NB, grown at 28°C for 12 h and then transferred onto plates containing NA and 10% sucrose. Sucrose-resistant colonies were replica streaked onto NA plates with and without kanamycin supplementation. Colonies resulting from double-crossover events were selected based on kanamycin-negative and sucrose-positive traits, and unmarked mutants were confirmed by PCR amplification of *hpa1* and *pthXo1*, respectively. To generate double mutants, pK18*sacB*:Δ*hpa1* was transformed into the Δ*pthXo1* mutant.

Different tags were attached to the 3′-terminus of *pthXo1* or *avrXa10* in the pZW*pthXo1* and pZW*avrXa10* plasmid vectors. To generate a *cya*-fused gene, 1218-bp *cya* fragment encoding amino acids 2–406 of the Cya protein were amplified from plasmid pMS107 and prefixed with the last 51-bp region of *pthXo1* that contained a *Sac*I recognition site. The recombinant sequence was inserted into pZW*pthXo1* at the *Sac*I site. A similar method was used for the construction of *avrXa10-cya*. To construct *pthXo1-blaM*, *blaM* was amplified from plasmid pBR322 using specific primers that contained a *Sal*I site. The confirmed PCR product was inserted into the *pthXo1* sequence at the *Sal*I site in pZW*pthXo1*, and *avrXa10-blaM* was similarly constructed (Makino *et al.* 2006). Every recombinant vector was linearized with *Hind*III and cloned into the pHM1 vector for genetic complementation. The *hpa1pthXo1* and *hpa1avrXa10* double-complementary vectors were constructed using two steps. First, the *hpa1* sequence that was linked to its own promoter was cloned into pHM1 between the *Pst*I and *Kpn*I sites. Second, pZW*avrXa10* or pZW*pthXo1* was linearized using *Hind*III and inserted into the *Hind*III site of pHM1*hpa1*. Complementation or transformation was performed by electroporation.

2.3 *BlaM reporter assay*

Rice protoplasts were prepared from aerial parts of 10–20-day-old Nipponbare seedlings according to previously described methods (Yoo *et al.* 2007), and BlaM reporter assays on rice protoplasts were conducted by following the technique established for animal-pathogenic bacteria (Mills *et al.* 2008). An aqueous washing and inoculation (WI) solution containing 0.5 M mannitol, 20 mM KCl and 4 mM 4-morpholineethanesulfonic acid with pH 5.7 was prepared. *Xoo* strains labeled with the *blaM* reporter gene were grown in XOM2 liquid medium to stimulate the T3 secretion system and to generate a preactivated culture. Preactivated bacterial cells were harvested and adjusted to an optical density (OD_{600}) of 1.0 using fresh XOM2 liquid medium. An equal volume of 2× WI was added to the bacterial suspensions, adjusting the bacterial dosage to OD_{600} of 0.5, followed by gentle shaking by hand. Rice protoplasts were prepared in the WI solution and a 45 μL aliquot of this suspension ($\sim 5 \times 10^4$ protoplasts) was treated with 5 μL of 10× CCF2/AM loading solution (CCF2/AM loading kit, Invitrogen) to reach 1 mM CCF2/AM final concentration in a well of a 96-well microplate. Mixtures were incubated for 60 min in the dark at room temperature and then for 15 min at 28°C. CCF2-labeled protoplasts were infected with bacterial cultures at a final density of ∼100 colony forming unit (cfu)/mL by dilution. Alternatively, bacterial cultures were supplemented with 1 mM of CCF2/AM and 0.3 mM of BlaM inhibitor as a component of the reagent kit. Immediately after protoplast infection, the microplate was placed in a plate reader (SpectramaMax M5, Molecular Devices), which was set at 28°C. Protoplasts were examined at an excitation wavelength of 405 nm and emission wavelengths of 450 and 535 nm at a 10 min interval until 200 minute-post incubation (mpi). The [P] value was calculated using

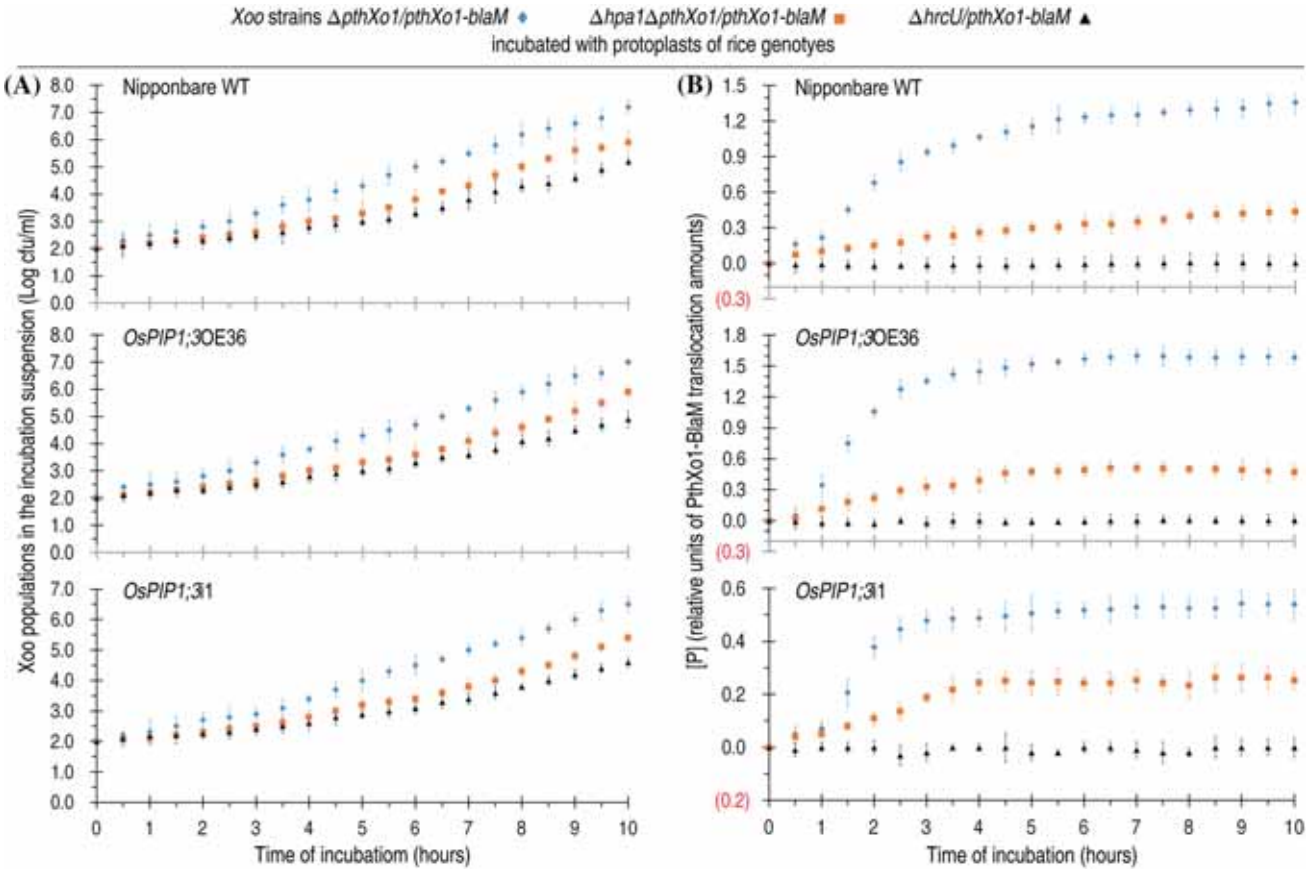

Figure 1. Multiplication of PthXo1-related *Xoo* strains in protoplasts and PthXo1-BlaM translocation into equivalent protoplasts of *OsPIP1;3*-related genotypes of the susceptible-rice variety Nipponbare. (**A**) Ten-hour monitoring records of population growth of the indicated *Xoo* strains in suspensions of incubation with protoplasts of the indicated plant genotypes. (**B**) Chronological changes of [P] concentrations, which indicate amounts of PthXo1-BlaM translocation into protoplasts. Data shown in (**A**) and (**B**) are mean values ± standard deviations (SDs) of results from three independent experiments (n = 3).

the formula [P] = ($P_{RAW} - P_{BEK}$)/S_0. Here, P_{RAW} refers to the measured product fluorescence at a wavelength of 450 nm; P_{BEK} is the background fluorescence at a wavelength of 450 nm (t = 0) and S_0 is the measured substrate fluorescence at 535 nm (t = 0). To visualize TALE-BlaM translocation, protoplasts were infected in an incubator at 28°C. After 100 min, protoplasts were examined by laser confocal microscopy using a green channel (535 nm) to capture fluorescence from intact CCF2, blue channel (450 nm) to visualize cleaved CCF2 and bright-field to observe protoplasts (Mills *et al.* 2013). In addition, bacterial multiplication during the investigation period was determined and quantified as cfu/mL, to verify the correlation of bacterial population with the level of effector translocation.

2.4 *Cya reporter assay*

AvrXa10 and PthXo1 were fused to the calmodulin-dependent adenylate-cyclase domain of CyaA as previously described (Wang *et al.* 2018). An increase in cAMP concentration in plant cells was then measured using an enzyme-linked immunosorbent assay (ELISA) kit. The Cya reporter assay was performed on 2-week-old rice seedlings inoculated with Cya-related *Xoo* strains. Bacterial suspensions were prepared from NA cultures and adjusted to a dosage of OD_{600} = 0.5. Each suspension was infiltrated into intercellular spaces of expanded leaves at three sites per leaf. At 9 h post-inoculation (hpi), 5-cm-long leaf segments that covered infiltration sites were excised from inoculated leaves, frozen in liquid nitrogen in a mortar and ground using a ceramic pestle to a fine powder. Leaf powders were transferred into a 1.5-mL tube and thawed with evaporation of liquid nitrogen. Thawed leaf powders in the tube were suspended using the isolation buffer from the cAMP ELISA detection kit (GenScript), followed by centrifugation at 12,000 rpm for 10 min. A part of the supernatant was used as soluble protein preparation, followed by immunoblotting using the anti-Cya antibody (Santa Cruz). Another part of the supernatant was amended with a solution of HCl at a final concentration of 0.1 M, followed by brief centrifugation. The newly produced supernatant was analyzed using the cAMP ELISA detection kit to determine intracellular cAMP concentrations in contrast to the amount of total proteins from a leaf sample. Total proteins in each sample for

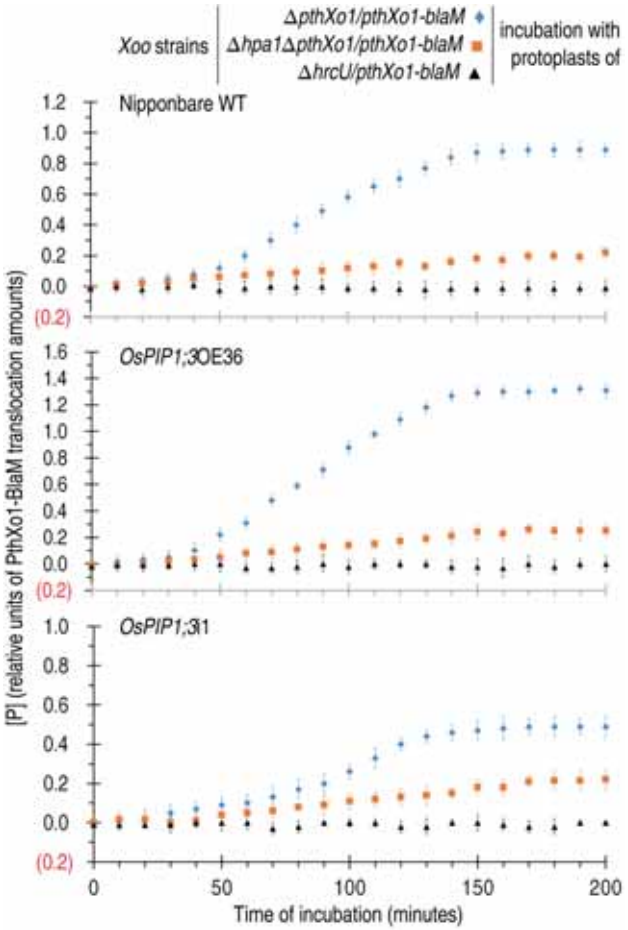

Figure 2. Real-time monitoring of PthXo1-BlaM translocation in the early stage (the first 200 min) of protoplast infection. Data shown are mean values ± SDs (n = 3 independent experiments).

normalization were quantified by using a BCA protein assay kit (TransGen Biotech).

2.5 *Gene-expression analysis*

Total RNA was isolated from plant leaves by using TRIzol (Invitrogen) and treated with DNase I (Invitrogen) to remove DNA, followed by cDNA synthesis by using a PrimeScript RT Master Mix (TaKaRa). Quantitative real-time reverse transcriptase PCR (RT-qPCR) analysis was performed in an ABI7500 Real-Time PCR system (Applied Biosystems) with a SYBR Premix Ex Taq kit (TaKaRa) using specific primers (supplementary table 2). The relative expression level of a tested gene was quantified as the gene to *Actin* transcript quantity ratio.

2.6 *Data treatment*

To guarantee comparability of quantitative data, all experiments were performed with equal quantities of plant or bacterial materials, as well as equal amounts/volumes of protein/nucleic acids and various reagents used in different analyses. All experiments were repeated at least three times with similar results. Quantitative data were analyzed by using the commercial IBM SPSS19.0 software package (Shi 2012). Homogeneity of variance in data was determined by the Levene test, and the formal distribution pattern of the data was confirmed by the Kolmogorov–Smirnov test and *P–P* plots. Analysis of variance and Duncan's multiple range tests were performed on data from at least three independent experiments each involving three repetitions.

3. Results

3.1 *Real-time monitoring of PthXo1-BlaM translocation*

The BlaM reporting assay was first performed using PthXo1-related recombinant PXO99^{A} strains and protoplasts of the susceptible-rice variety Nipponbare. Protoplasts were incubated with a low-bacterial dosage, ∼100 cfu per milliliter, of the strain Δ*pthXo1/pthXo1-blaM*, Δ*hpa1*Δ*pthXo1/pthXo1-blaM* or Δ*hrcU/pthXo1-blaM*, which were generated previously (Wang *et al.* 2018; Zhang *et al.* 2018; Li *et al.* 2019). Bacterial multiplication in the incubation suspension (figure 1A) and protoplast import of the PthXo1-BlaM fusion protein, shown as [P] values over the background readings scored at 0 mpi (figure 1B), were monitored at 30-min intervals in 10 h post-incubation (hpi). During this period, populations of the different strains were increased from the initial amount of ∼200–10^{5-7} cfu/mL, suggesting sufficient multiplication of bacteria in the system (figure 1A). Accompanying bacterial population growth, substantial translocation of the PthXo1-BlaM fusion protein was detected since 1 hpi; translocation quantity was increased in 5 hpi and then remained constant up to 10 hpi (figure 1B). In 10 hpi, the translocation amount of PthXo1-BlaM was reduced markedly by deletion of Hpa1, as observed with the strain Δ*hap1*Δ*pthXo1/pthXo1-blaM* while no translocation was found in protoplasts incubated with the Δ*hrcU/pthXo1-blaM* mutant (figure 1B). These data indicate that the BlaM reporter is feasible in assessing the PthXo1 translocator and the negative effects of Hpa1 and HrcU (Wang *et al.* 2018).

The feasibility of the BlaM reporter for the *Xoo*–Nipponbare compatible interaction was confirmed by quantifying differences of PthXo1-BlaM translocation into protoplasts of WT Nipponbare, *OsPIP1;3*OE36 and *OsPIP1;3*i1 plants. PthXo1-BlaM translocation quantities were highly increased by *OsPIP1;3*OE36 but decreased by *OsPIP1;3*i1 compared to the WT. In different plants, the protoplast import of PthXo1-BlaM (figure 1B) was coincident with bacterial multiplication during 10 hpi (figure 1A). Thus, the BlaM reporting system can be used to detect

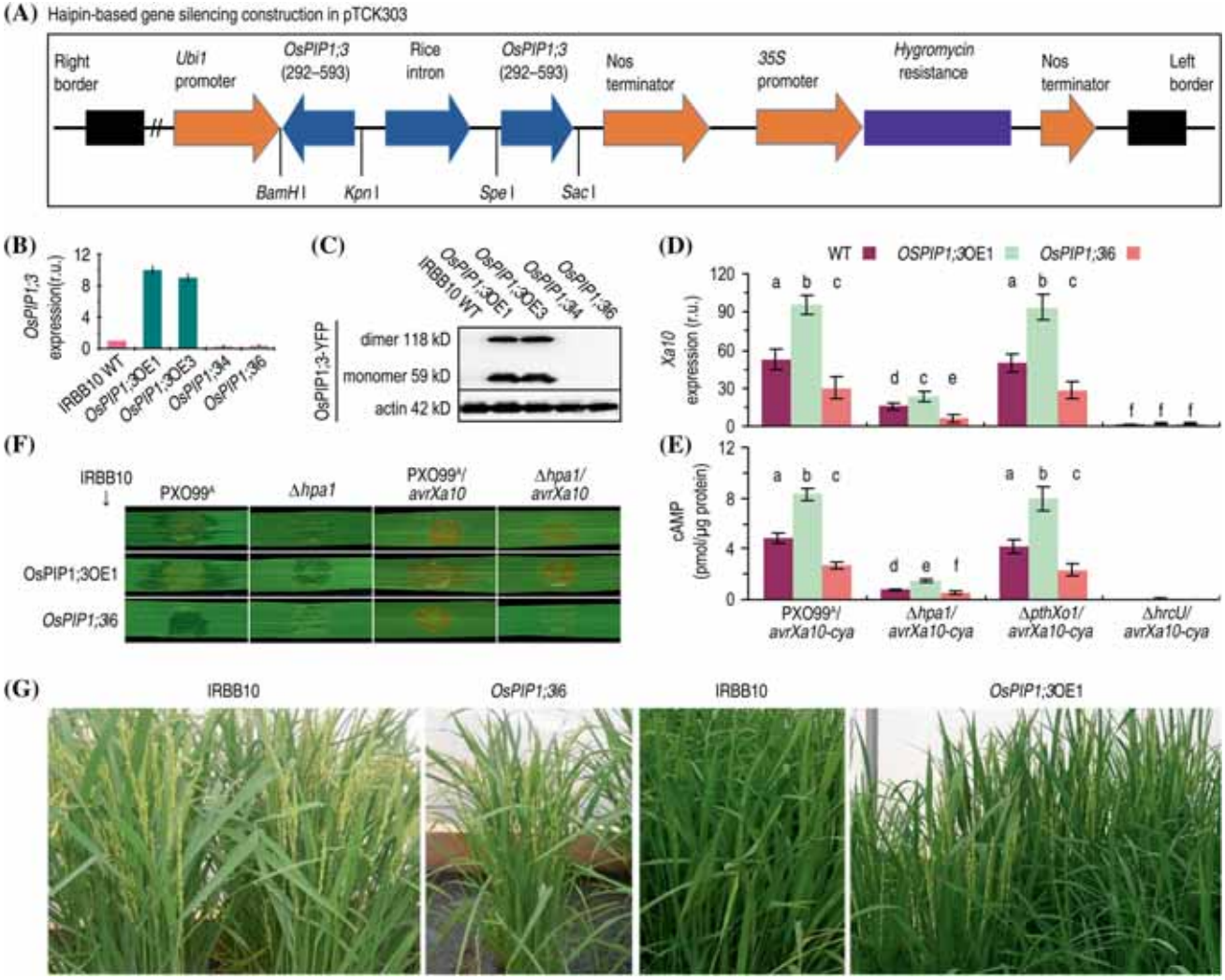

Figure 3. Genetic modifications of the *OsPIP1;3* gene and the subsequent effects on AvrXa10 translocation and pathological performance. (**A**) The hairpin construct used to silence the *OsPIP1;3* gene under the IRBB10 background. (**B**) Real-time RT-PCR analysis of OsPIP1;3 expression difference in the different plants. Data shown are mean values ± SDs (n = 6 independent experiments). (**C**) Immunoblotting of leaf PM proteins probed by hybridization with the specific anti-YFP antibody. (**D**) and (**E**) Different levels of *Xa10* expression and AvrXa10-Cya translocation in the three plants at 9 h post-inoculation with the *Xoo* strains shown on the bottom. (**F**) Fragments of leaves photographed after 5 days of plant inoculation by the leaf-infiltration method. (**G**) T3 progenies of the transgenic plants reproduced together with WT IRBB10. Data shown in (**B**), (**D**) and (**E**) are mean values ± SDs (n = 5 independent experiments).

real-time variations of the effector translocation, as analyzed at 30 min intervals during 10 hpi, which covers several cycles of bacterial multiplication.

To further validate the real-time monitoring feature of the BlaM reporter in detecting PthXo1 translocation, chronological changes of [P] (PthXo1-BlaM translocation) quantities were determined at a short (10 min) interval within a short period, 200 mpi (figure 2). In this period, bacterial populations were increased approximately by 10 times (figure 1A), accompanying PthXo1-BlaM translocation with a detectable level at different times in WT Nipponbare, *OsPIP1;3*OE36 and *OsPIP1;3*i1 plants. On the one hand, the effects of *OsPIP1;3* overexpression and silencing on PthXo1-BlaM translocation were characterized as the time to evident increases in [P] concentrations over the background readings scored at 0 mpi, and the time at 60, 50 and 80 mpi in the WT, *OsPIP1;3*OE36 and *OsPIP1;3*i1, respectively (figure 2). On the other, the effects of *OsPIP1;3* overexpression and silencing on PthXo1-BlaM translocation were found as the difference in the [P] amounts. Surely after 80 mpi, the values of PthXo1-BlaM translocation (levels of [P] production) were higher in *OsPIP1;3*OE36 but lower in *OsPIP1;3*i1 compared to WT Nipponbare (figure 2). Moreover, PthXo1-BlaM translocation found at each time point in 200 mpi was reduced by deleting the *hap1* gene from the bacterial genome and eliminated by deletion of *hrcU*. Therefore, the BlaM reporter is effective at detecting the chronological changes of PthXo1 translocation at intervals as short as 10 min within the early stage of bacterial multiplication.

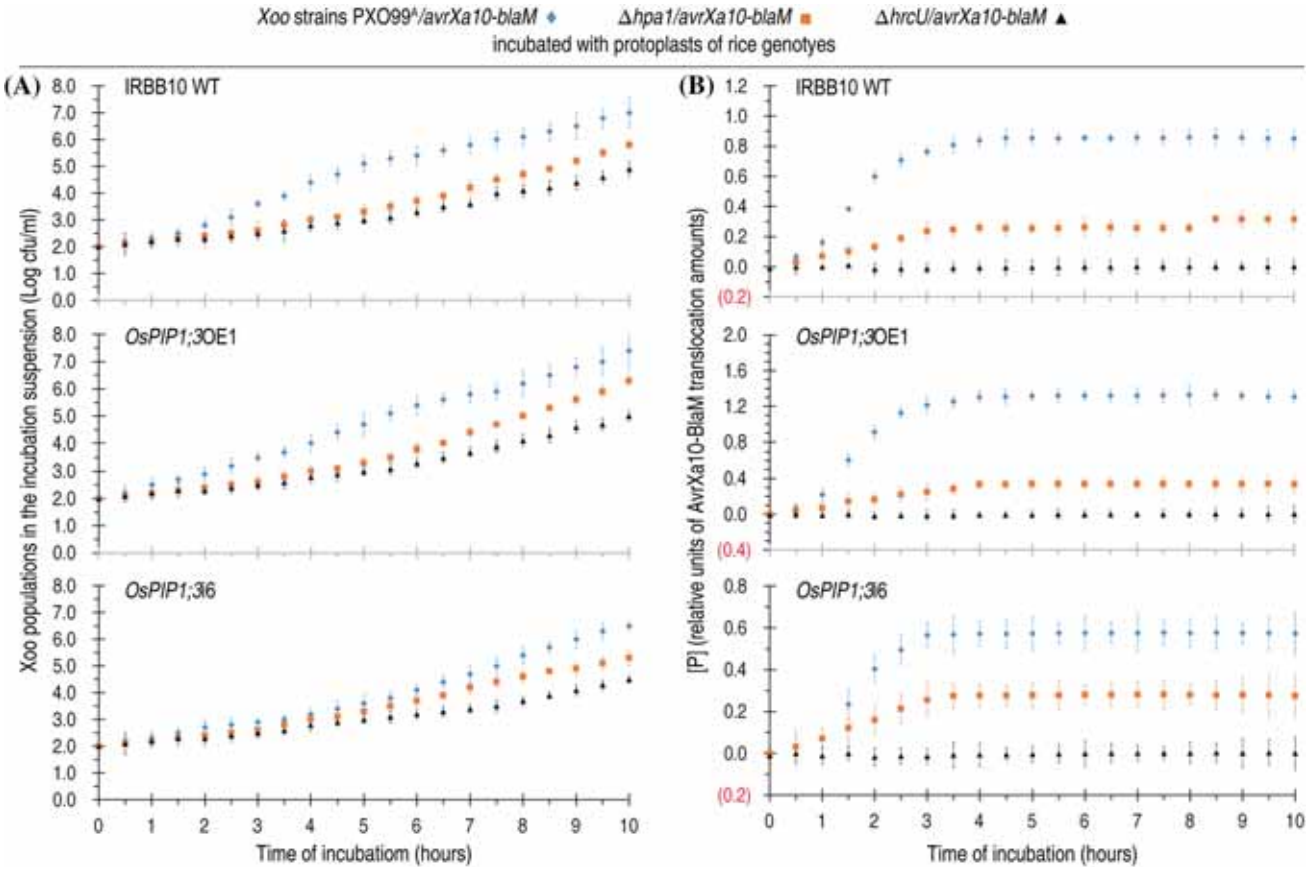

Figure 4. Multiplication of AvrXa10-related *Xoo* strains in protoplasts and AvrXa10-BlaM translocation into equivalent protoplasts of *OsPIP1;3*-related genotypes of the susceptible-rice variety IRBB10. (**A**) Ten-hour monitoring records of population growth of the indicated *Xoo* strains in suspensions of incubation with protoplasts of the indicated plant genotypes. (**B**) Chronological changes of [P] concentrations, which indicate amounts of AvrXa10-BlaM translocation into protoplasts. Data shown in (**A**) and (**B**) are mean values ± standard deviations of results from three independent experiments (n = 3).

3.2 *OsPIP1;3 overexpression and silencing*

Recently, we used the Cya reporting system to determine the translocation of the *Xoo*'s TALE AvrXa10. This TALE was introduced into PXO99^{A} from the *Xoo* strain PXO86 and was found to move from the recombined PXO99^{A} strain PXO99^{A}/*avrXa10-blaM* into cells of IRBB10, a rice variety susceptible to PXO99^{A} (Wang *et al.* 2018). In the present study, we determined AvrXa10 translocation by using the BlaM reporter applied to the WT IRBB10, *OsPIP1;3*OE and *OsPIP1;3*i lines. We generated *OsPIP1;3*-overexpression transgenic IRBB10 lines (supplementary figure 1) by transformation with *OsPIP1;3* fused to the gene encoding yellow-fluorescent protein (YFP) and a constitutive promoter (supplementary figure 1). We also generated the *OsPIP1;3*-silenced line of IRBB10 (supplementary figure 1) by a hairpin construct (figure 3A). In the WT IRBB10, the recombinant strain PXO99^{A}/*avrXa10-blaM* plays an avirulence role and causes the hypersensitive response (HR). Compared to the level in WT IRBB10, the HR acquired a higher degree in *OsPIP1;3*OE plants but incurred significant (P<0.01) impairment by *OsPIP1;3*i (supplementary figure 2A). Consistently, the host susceptibility gene *Xa10*, the target of *AvrXa10* (Tian *et al.* 2014), was highly expressed in WT IRBB10 markedly enhanced by *OsPIP1;3*OE but significantly (P<0.01) inhibited in *OsPIP1;3*i lines (supplementary figure 2B).

3.3 *OsPIP1;3 and Hpa1 cooperation in AvrXa10 translocation*

Two *OsPIP1;3*-overexpressing lines (*OsPIP1;3*OE1 and *OsPIP1;3*OE3) and two *OsPIP1;3*-silencing lines (*OsPIP1;3*i4 and *OsPIP1;3*i6) were further studied in comparison with the WT plant (figure 3B). The gene over-expression or silencing was confirmed (figure 3B), and production of the OsPIP1;3-YFP fusion protein was detected only in *OsPIP1;3*OE1 and *OsPIP1;3*OE3 (figure 3C). The different plants were inoculated by leaf infiltration with bacterial suspensions of PXO99^{A}/*avrXa10-cya*, Δ*hpa1*/*avrXa10-cya*, Δ*pthXo1*/*avrXa10-cya* and Δ*hrcU*/*avrXa10-cya*, respectively. In the subsequent 9 hpi, high levels of both *Xa10* expression (figure 3D) and AvrXa10-Cya translocation

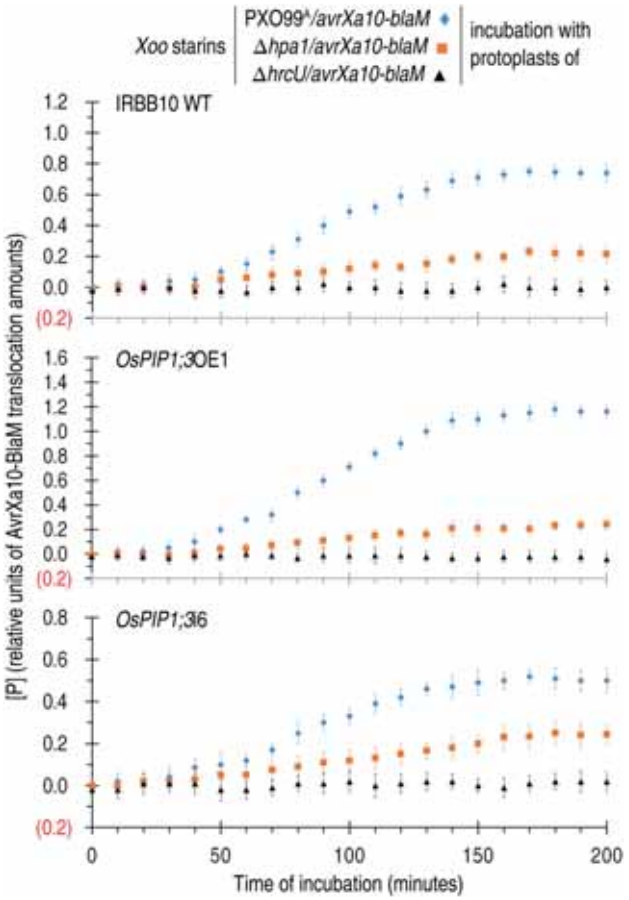

Figure 5. Real-time monitoring of AvrXa10-BlaM translocation in the early stage (the first 200 min) of protoplast infection. Data shown are mean values ± SDs (n = 3 independent experiments).

(cytoplasmic cAMP; figure 3E) were detected in WT plants inoculated with PXO99^{A}/*avrXa10-cya* or Δ*pthXo1/avrXa10-cya*. This suggests that AvrXa10 and PthXo1 act independently in the translocation and virulence performance. However, *Xa10* expression and AvrXa10-Cya translocation were significantly (P<0.01) decreased by Δ*hpa1/avrXa10-cya*, suggesting the important role of *hpa1* in the virulence performance. Moreover, *Xa10* expression and AvrXa10-Cya translocation were canceled by Δ*hrcU/avrXa10-cya*, confirming the critical function of *hrcU*. Furthermore, the levels of *Xa10* expression (figure 3D) and AvrXa10-Cya translocation (figure 3E) were concomitantly increased by *OsPIP1;3* overexpression but decreased when *OsPIP1;3* was silenced. *OsPIP1;3* overexpression resulted in aggravated virulence of PXO99^{A}, or the increased avirulence of PXO99^{A}/*avrXa10* (figure 3F). By contrast, the virulence or avirulence was comprised of *OsPIP1;3* silencing. Based on these results, Hpa1 cooperates with OsPIP1;3 to support *Xa10* expression, AvrXa10 translocation, as well as the virulence or avirulence. Therefore, both genotypes of transgenic plants were further reproduced (figure 3G) for use in BlaM reporter assays of AvrXa10.

3.4 *Real-time monitoring of AvrXa10-BlaM translocation*

Protoplasts of WT IRBB10, *OsPIP1;3*OE1 and *OsPIP1;3*i6 were incubated with a suspension of the *Xoo* strain PXO99^{A}/*avrXa10-blaM*, Δ*hpa1/avrXa10-blaM* or Δ*hrcU/avrXa10-blaM*, followed by monitoring of bacterial populations (figure 4A) and AvrXa10-BlaM moved into protoplasts (figure 4B) at 30-min intervals in 10 hpi. In the incubation suspension of WT protoplasts, bacterial populations were increased since 2 hpi, with PXO99^{A}/*avrXa10-blaM* having higher amount at each time point. By contrast, bacterial populations of Δ*hpa1/avrXa10-blaM* remained as low as Δ*hrcU/avrXa10-blaM* not until 5.5 hpi. In agreement with the changes of bacterial populations, AvrXa10-BlaM translocation was detectable since 2 hpi from PXO99^{A}/*avrXa10-blaM*, which successively supported the protein translocation. In comparison, AvrXa10-BlaM translocation was delayed by 2 h in the case of Δ*hpa1/avrXa10-blaM*, which was less vigorous than PXO99^{A}/*avrXa10-blaM* in facilitating the protein translocation. This analysis suggests that the BlaM reporter is reliable in quantifying the protoplast import of AvrXa10 under mediation by Hpa1.

The feasibility of the BlaM reporter for the *Xoo*-IRBB10 incompatible interaction was confirmed by quantifying differences of AvrXa10-BlaM translocation into protoplasts of WT Nipponbare, *OsPIP1;3*OE1 and *OsPIP1;3*i6 plants. AvrXa10-BlaM translocation quantities were highly increased by *OsPIP1;3*OE1 but decreased by *OsPIP1;3*i6 compared to the WT plant. In different plants, the protoplast import of AvrXa10-BlaM (figure 4B) was coincident with bacterial multiplication during 10 hpi (figure 4A). Hence, the BlaM reporting system can be used to detect real-time variations of the effector translocation, as analyzed at 30 min intervals in 10 hpi, which covers several cycles of bacterial multiplication.

To further validate the real-time monitoring feature of the BlaM reporter in detecting AvrXa10 translocation, chronological changes of [P] (AvrXa10-BlaM translocation) quantities were determined at a short (10 min) interval within a short period, 200 mpi (figure 5). In this period, bacterial populations were increased nearby 10 times (figure 4A), accompanying AvrXa10-BlaM translocation with a detectable level at different times in WT IRBB10, *OsPIP1;3*OE1 and *OsPIP1;3*i6 plants. In the initial stage of incubation, the effects of *OsPIP1;3* overexpression and silencing on AvrXa10-BlaM translocation were shown as the time to evident increases in [P] concentrations over the background readings scored at 0 mpi, and the time was 60, 50 and 70 mpi in the WT, *OsPIP1;3*OE1 and *OsPIP1;3*i6, respectively (figure 5). Subsequently, the effects of *OsPIP1;3* overexpression and silencing on AvrXa10-BlaM translocation were determined as the difference in the [P] amounts. Surely after 70 mpi, values of AvrXa10-BlaM translocation (levels of [P] production) were higher in *OsPIP1;3*OE1 but lower in *OsPIP1;3*i6 compared to WT

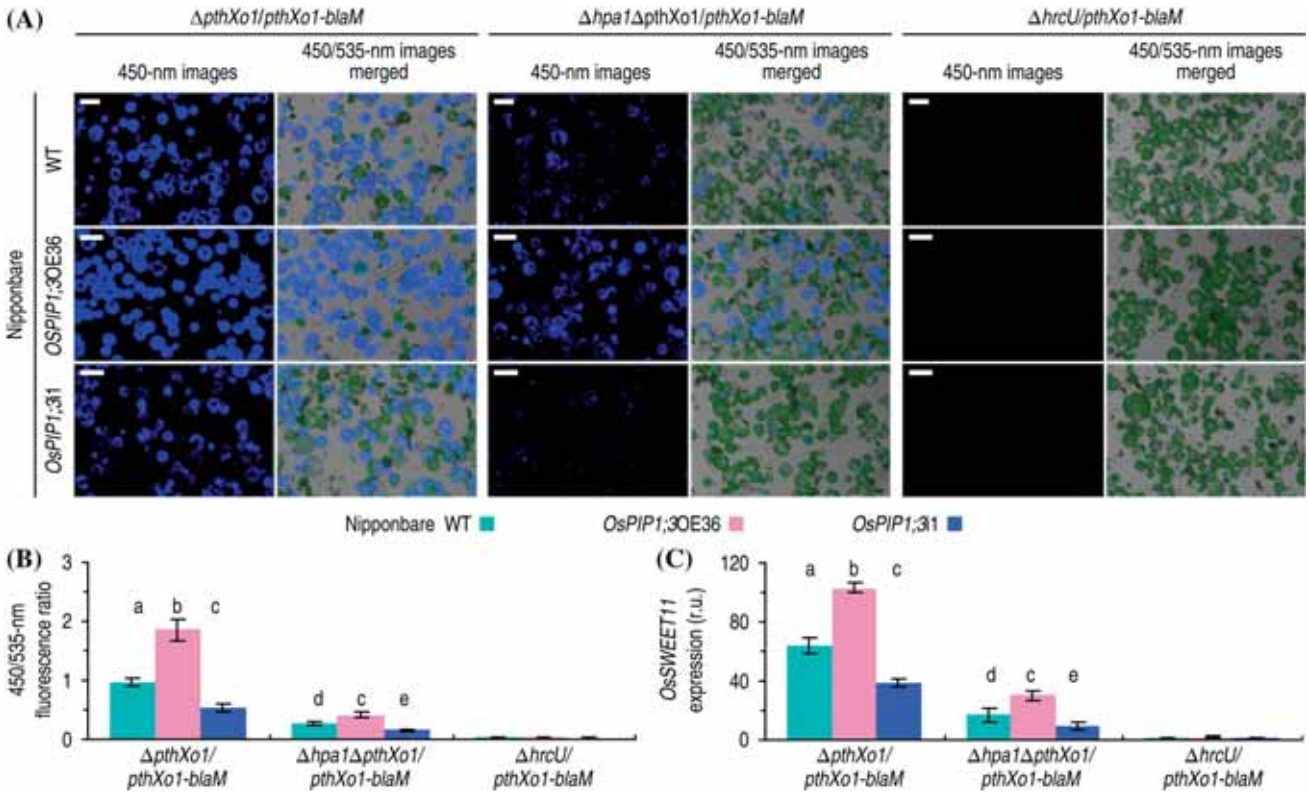

Figure 6. Visualization of PthXo1-BlaM translocation and *OsSWEET11* expression in protoplast in *OsPIP1;3*-related genotypes of Nipponbare. (**A**) Microscopy imaging of rice protoplasts after 100 mpi, that is, 100 min of incubation with bacterial cells of *Xoo* strains indicated on top. Protoplasts were emitting blue and green fluorescence with and without translocated PthXo1-BlaM, respectively. Scale bars = 50 μm. (**B**) Green-to-blue fluorescence density ratios in protoplasts from B based on automatic analysis with the MetaMorph software. (**C**) *OsSWEET11* expression in protoplasts at 200 mpi. The average expression level of *SWEET11* in Nipponbare with Δ*hrcU*/*pthXo1-blaM* was defined as 1 to evaluate relative extents of gene expression in other plants. In (**B**) and (**C**), data are the means ± SD; different letters on bar graphs indicate significant differences among data from the different combinations of plants and bacterial strains; $P<0.05$; $n = 9$ repetitions from three independent experiments each involving three repetitions.

IRBB10 (figure 5). Furthermore, AvrXa10-BlaM translocation found at each time point in 200 mpi was reduced by deleting the *hap1* gene from the bacterial genome and eliminated by deletion of *hrcU*. Therefore, the BlaM reporter is effective at detecting the chronological changes of AvrXa10 translocation at intervals short of 10 min within the early stage of bacterial multiplication.

3.5 *Imaging of TALE-BlaM transport*

Fluorescence imaging showed that more *OsPIP1;3*OE36 protoplasts contained PthXo1-BlaM, whereas a small proportion of *OsPIP1;3*i1 protoplasts contained the protein (figure 6A). Ratios of green-to-blue fluorescence densities were greater in *OsPIP1;3*OE36, but smaller in *OsPIP1;3*i1 protoplast populations compared to the ratio of WT protoplasts (figure 6B). While *OsPIP1;3*OE36 resulted in the upregulation of *OsSWEET11* expression, *OsPIP1;3*i1 protoplasts resulted in reduction of *OsSWEET11* expression compared to that observed in the WT (figure 6C). Similarly, the proportion of protoplasts that accommodated AvrXa10-BlaM increased with *OsPIP1;3*OE1, but decreased with the gene *OsPIP1;3*i6 (figure 7A and B). In concert with the change of AvrXa10 translocation, *Xa10* expression was enhanced and weakened by *OsPIP1;3*OE1 and *OsPIP1;3*i6, respectively (figure 7C). In addition, PthXo1 and AvrXa10 seemed to be translocated equally well in the protoplast system (figure 6A compared with figure 7A).

4. Discussion

Because of convenient operation with the plate reader and automatic monitoring of [P], the BlaM reporting system is able to provide readings at any designed interval during infection of eukaryotic cells or protoplasts by a bacterial pathogen (Mueller *et al.* 2008). Because of the FRET changes derived from the BlaM hydrolytic substrate CCF2, the BlaM reporter allows for visualizing eukaryotic cells or protoplasts that have accommodated a BlaM-fused prokaryotic effector translocated already (Jones and Padilla-

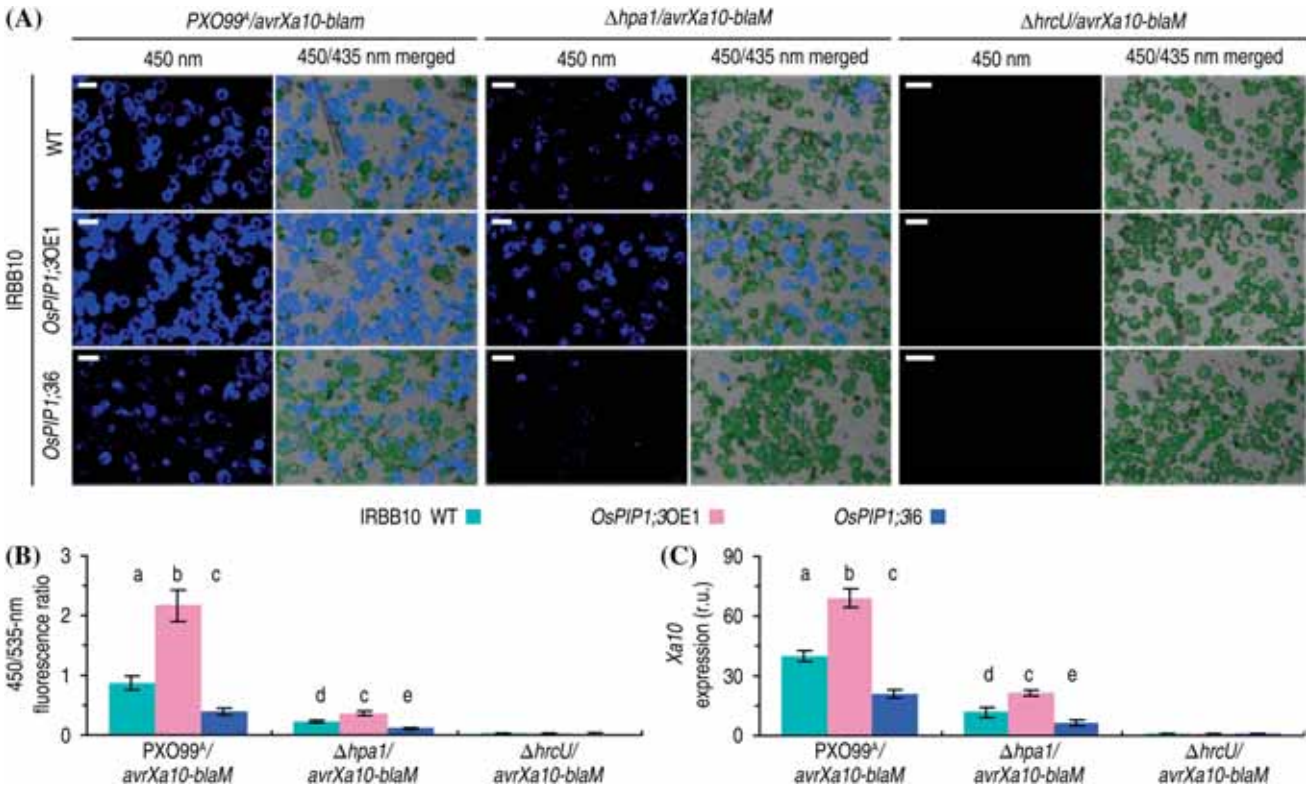

Figure 7. Visualization of AvrXa10-BlaM translocation and *Xa10* expression in protoplast in *OsPIP1;3*-related genotypes of IRBB10. (**A**) Microscopy imaging of rice protoplasts after 100 mpi, that is, 100 min of incubation with bacterial cells of *Xoo* strains indicated on top. Protoplasts were emitting blue and green fluorescence with and without translocated AvrXa10-BlaM, respectively. Scale bars = 50 μm. (**B**) Green-to-blue fluorescence density ratios in protoplasts from (**B**) based on automatic analysis with the MetaMorph software. (**C**) *Xa10* expression in protoplasts at 200 mpi. The average expression level of *Xa10* in IRBB10 with Δ*hrcU*/*avrXa10-blaM* was defined as 1 to evaluate relative extents of gene expression in other plants. In (**B**) and (**C**), data are the means ± SD; different letters on bar graphs indicate significant differences among data from the different combinations of plants and bacterial strains; $P<0.05$; $n = 9$ repetitions from three independent experiments each involving three repetitions.

Parra 2016). With the technical merits, the BlaM reporter system initially established for animal-pathogenic bacteria (Mueller *et al.* 2008) has been extended to a plant pathogen in this study. The effects of Hpa1 and OsPIP1;3 on the TALE translocation were elucidated previously (Wang *et al.* 2018; Zhang *et al.* 2018) and were used to evaluate the feasibility of the protoplast BlaM reporting system in the study of plant-pathogenic bacteria.

We have described a straightforward case study on the use of the BlaM reporter in monitoring of PthXo1 and AvrXa10 translocation from *Xoo* cells into protoplasts of the susceptible- and resistant-rice varieties Nipponbare and IRBB10, respectively. Real-time quantification and microscopic visualization of TALE-BlaM fusion proteins confirm the technical advantage of the BlaM reporting system over the conventional Cya reporter, which has experimental limitations for chronological and imaging analyses of effector translocation (Kvitko *et al.* 2007; Bocsanczy *et al.* 2008; Wang *et al.* 2018; Zhang *et al.* 2018). The technical advantages that the BlaM reporter possesses have been demonstrated by evaluating the effects of Hpa1 and OsPIP1;3 on the translocation of TALE-BlaM fusion proteins. Moreover, the protoplast BlaM reporting system can be used to analyze the expression of *OsSWEET11* and *Xa10*, which are targets of PthXo1 and AvrXa10 (Yang *et al.* 2006; Tian *et al.* 2014) and are expressed as a consequence of the effector translocation in protoplasts. Furthermore, quantities of translocated effector-BlaM fusion proteins are correlated with densities of blue fluorescence originated from the hydrolytic activity of BlaM, providing a convenient method to visualize protoplasts containing translocated effector-BlaM fusion proteins. It seems that PthXo1 and AvrXa10 can be translocated equally well in the protoplast BlaM system, which, however, allows for estimating relative levels of translocated effectors.

These demonstrations indicate that the BlaM reporter system can provide real-time, high-throughput monitoring of bacterial effector translocation into plant protoplasts. In addition, the application of the BlaM reporter to plant protoplasts can be used to analyze induced expression of the effector target gene. Therefore, the protoplast BlaM reporting system can be used not only for monitoring of effector

translocation, but also for the subsequent virulence (avirulence) performance. It is necessary to further extend the system to more species of plants and plant-pathogenic bacteria.

Acknowledgements

We thank Professor Bing Yang (Department of Genetics, Development, and Cell Biology, Iowa State University) for the gift of the *pthXo1* vector and our colleague Professor Ling Jiang (Agronomy College, Nanjing Agricultural University) for assistance in rice transformation. We thank financial support from the China National Key Research and Development Plan (Grant Number 2017YFD0200901), Natural Science Foundation of China (Grant Number 31772247) and Talent Recruitment Funding of Shandong Agricultural University (Grant Number 20171226).

References

Alfano JR and Collmer A 2004 Type III secretion system effector proteins: Double agents in bacterial disease and plant defense. *Annu. Rev. Phytopathol.* **42** 385–414

Bocsanczy AM, Nissinen RM, Oh CS and Beer SV 2008 Hrpn of *Erwinia amylovora* functions in the translocation of DspA/E into plant cells. *Mol. Plant Pathol.* **9** 425–434

Bogdanove AJ and Voytas DF 2011 TAL effectors: Customizable proteins for DNA targeting. *Science* **333** 1843–1846

Büttner D 2012 Protein export according to schedule: Architecture, assembly, and regulation of type III secretion systems from plant- and animal-pathogenic bacteria. *Microbiol. Mol. Biol. Rev.* **76** 262–310

Chakravarthy S, Huot B and Kvitko BH 2017 Effector translocation: Cya reporter assay. *Methods Mol. Biol.* **1615** 473–487

Charkowski AO, Alfano JR, Preston G, Yuan J, He SY and Collmer A 1998 The *Pseudomonas syringae* pv. *tomato* hrpw protein has domains similar to harpins and pectate lyases and can elicit the plant hypersensitive response and bind to pectate. *J. Bacteriol.* **180** 5211–5217

Chatterjee S, Chaudhury S, McShan AC, Kaur K and De GR 2013 Structure and biophysics of type III secretion in bacteria. *Biochemistry* **52** 2508–2517

Chen H, Chen J, Li M, Chang M, Xu K, Shang Z, Zhao Y, Palmer I, Zhang Y, McGill J, Alfano JR, Nishimura MT, Liu F and Fu ZQ 2017 A bacterial type III effector targets the master regulator of salicylic acid signalling, NPR1, to subvert plant immunity. *Cell Host Microbe* **22** 777–788

Chen L, Qian J, Qu S, Long J, Yin Q, Zhang C, Wu X, Sun F, Wu T, Hayes M, Beer SV and Dong H 2008 Identification of specific fragments of $HpaG_{Xooc}$, a harpin protein from *Xanthomonas oryzae* pv. *oryzicola*, that induce disease resistance and enhanced growth in rice. *Phytopathology* **98** 781–791

Choi MS, Kim W, Lee C and Oh CS 2013 Harpins, multifunctional proteins secreted by gram-negative plant-pathogenic bacteria. *Mol. Plant-Microbe Interact.* **26** 1115–1122

Dik DA, Marous DR, Fisher JF and Mobashery S 2017 Lytic transglycosylases: Concinnity in concision of the bacterial cell wall. *Crit. Rev. Biochem. Mol. Biol.* **52** 503–542

Domingues L, Ismail A, Charro N, Rodríguez-Escudero I, Holden DW, Molina M, Cid VJ and Mota LJ 2016 The *Salmonella* effector SteA binds phosphatidylinositol 4-phosphate for subcellular targeting within host cells. *Cell. Microbiol.* **18** 949–969

Dong N, Niu M, Hu L, Yao Q, Zhou R and Shao F 2016 Modulation of membrane phosphoinositide dynamics by the phosphatidylinositide 4-kinase activity of the *Legionella* lepb effector. *Nat. Microbiol.* **12** 16236

Finsel I and Hilbi H 2015 Formation of a pathogen vacuole according to *Legionella pneumophila*: How to kill one bird with many stones. *Cell. Microbiol.* **17** 935–950

Gu Y, Zavaliev R and Dong X 2017 Membrane trafficking in plant immunity. *Mol. Plant* **10** 1026–1034

Haapalainen M, Engelhardt S, Küfner I, Li CM, Nürnberger T, Lee J, Romantschuk M and Taira S 2011 Functional mapping of harpin HrpZ of *Pseudomonas syringae* reveals the sites responsible for protein oligomerization, lipid interactions and plant defence induction. *Mol. Plant Microbe Interact.* **12** 151–166

Hartmann N and Büttner D 2013 The inner membrane protein HrcV from *Xanthomonas* spp. is involved in substrate docking during type III secretion. *Mol. Plant Microbe Interact.* **26** 1176–1189

Ji H and Dong H 2015a Biological significance and topological basis of aquaporin-partnering protein-protein interactions. *Plant Signaling Behav.* **10** e1011947

Ji H and Dong H 2015b Key steps in type III secretion system (T3SS) towards translocon assembly with potential sensor at plant plasma membrane. *Mol. Plant Pathol.* **16** 762–773

Jones DM and Padilla-Parra S 2016 The β-lactamase assay: Harnessing a FRET biosensor to analyse viral fusion mechanisms. *Sensors (Basel). https://doi.org/10.3390/s16070950*

Kikuchi Y, Hijikata N, Ohtomo R, Handa Y, Kawaguchi M, Saito K, Masuta C and Ezawa T 2016 Aquaporin-mediated long-distance polyphosphate translocation directed towards the host in arbuscular mycorrhizal symbiosis: Application of virus-induced gene silencing. *New Phytol.* **211** 1202–1208

Kim JF and Beer SV 1998 Hrpw of *Erwinia amylovora*, a new harpin that contains a domain homologous to pectate lyases of a distinct class. *J. Bacteriol.* **180** 5203–5210

Kvitko BH, Ramos AR, Morello JE, Oh HS and Collmer A 2007 Identification of harpins in *Pseudomonas syringae* pv. *tomato* DC3000, which are functionally similar to HrpK1 in promoting translocation of type III secretion system effectors. *J. Bacteriol.* **189** 8059–8072

Li YR, Che YZ, Zou HS, Cui YP, Guo W, Zou LF, Biddle EM, Yang CH and Chen GY 2011 Hpa2 required by HrpF to translocate *Xanthomonas oryzae* transcriptional activator-like effectors into rice for pathogenicity. *Appl. Environ. Microbiol.* **11** 3809–3818

Li P, Zhang LY, Mo XY, Ji HT, Bian HJ, Hu YQ, Majid T, Long JY, Pang H, Tao Y, Ma JB and Dong HS 2019 Aquaporin PIP1;3 of rice and harpin Hpa1 of bacterial blight pathogen cooperate in a type III effector translocation. *J. Exp. Bot.* **pii** erz130

Makino S, Sugio A, White F and Bogdanove AJ 2006 Inhibition of resistance gene-mediated defense in rice by *Xanthomonas oryzae* pv. *oryzicola*. *Mol. Plant Microbe Interact.* **19** 240–249

Mills E, Baruch K, Charpentier X, Kobi S and Rosenshinea I 2008 Real-time analysis of effector translocation by the type III secretion system of enteropathogenic *Escherichia coli*. *Cell Host Microbe* **3** 104–113

Mills E, Baruch K, Aviv G, Nitzan M and Rosenshinea I 2013 Dynamics of the type III secretion system activity of enteropathogenic *Escherichia coli*. *MBio.* **4** e00303–e00313

Mueller CA, Broz P and Cornelis GR 2008 The type III secretion system tip complex and translocon. *Mol. Microbiol.* **68** 1085–1095

Scheibner F, Marillonnet S and Büttner D 2017 The TAL effector AvrBs3 from *Xanthomonas campestris* pv. *vesicatoria* contains multiple export signals and can enter plant cells in the absence of the type III secretion translocon. *Front. Microbiol.* **8** 2180

Schreiber KJ, Baudin M, Hassan JA and Lewis JD 2016 Die another day: Molecular mechanisms of effector-triggered immunity elicited by type III secreted effector proteins. *Semin. Cell Dev. Biol.* **56** 124–133

Shi LW 2012 *SPSS19.0 statistical analysis from accidence to conversance* (Beijing: Tsinghua University Press) pp 109–143

Tian D, Wang J, Zeng X, Gu K, Qiu C, Yang X, Zhou Z, Goh M, Luo Y, Murata-Hori M, White FF and Yin Z 2014 The rice TAL effector-dependent resistance protein XA10 triggers cell death and calcium depletion in the endoplasmic reticulum. *Plant Cell* **26** 497–515

Wang X, Ji H, Mo X, Zhang L, Li P, Wang J and Dong H 2018 Hpa1 is a type III translocator in *Xanthomonas oryzae* pv. *oryzae*. *BMC Microbiol.* **18** 105

White FF, Potnis N, Jones JB and Koebnik R 2009 The type III effectors of *Xanthomonas*. *Mol. Plant Pathol.* **10** 749–766

Yang B, Sugio A and White FF 2006 Os8n3 is a host disease-susceptibility gene for bacterial blight of rice. *Proc. Natl. Acad. Sci. USA* **103** 10503–10508

Yoo S, Cho YH and Sheen J 2007 Arabidopsis mesophyll protoplasts, a versatile cell system for transient gene expression analysis. *Nat. Protoc.* **2** 1565–1572

Zhang J, Yin Z and White F 2015 TAL effectors and the executor *R* genes. *Front. Plant Sci.* **6** 641

Zhang L, Hu Y, Li P, Wang X and Dong H 2018 Silencing of an aquaporin gene diminishes bacterial blight disease and enhances host resistance in rice. *Australas. Plant Pathol. https://doi.org/10.1007/s13313-018-0609-1*

Zhu WG, MaGbanua MM and White FF 2000 Identification of two novel *hrp*-associated genes in the hrp gene cluster of *Xanthomonas oryzae* pv. *oryzae*. *J. Bacteriol.* **182** 1844–1853

Corresponding editor: Ashis Kumar Nandi